Novel *Campylobacter concisus* lipooligosaccharide is a determinant of inflammatory potential and virulence[s]

Katja Brunner,[1,2,*] Constance M. John,[2,†,§] Nancy J. Phillips,[**] Dagmar G. Alber,[*] Matthew R. Gemmell,[††] Richard Hansen,[§§] Hans L. Nielsen,[***,†††] Georgina L. Hold,[§§§] Mona Bajaj-Elliott,[*] and Gary A. Jarvis[3,†,§]

Infection, Immunity and Inflammation Programme,[*] University College London Great Ormond Street Institute of Child Health, London, United Kingdom; Center for Immunochemistry,[†] Veterans Affairs Medical Center, San Francisco, CA; Department of Laboratory Medicine[§] and Department of Pharmaceutical Chemistry,[**] University of California, San Francisco, CA; Center for Genome-Enabled Biology and Medicine,[††] School of Medicine, Medical Sciences and Nutrition, Institute of Medical Sciences, University of Aberdeen, Aberdeen, United Kingdom; Department of Paediatric Gastroenterology,[§§] Royal Hospital for Children, Glasgow, United Kingdom; Department of Infectious Diseases[***] and Department of Clinical Microbiology,[†††] Aalborg University Hospital, Aalborg, Denmark; and St George and Sutherland Clinical School,[§§§] University of New South Wales, Sydney, Australia

Abstract The pathogenicity of *Campylobacter concisus*, increasingly found in the human gastrointestinal (GI) tract, is unclear. Some studies indicate that its role in GI conditions has been underestimated, whereas others suggest that the organism has a commensal-like phenotype. For the entero-pathogen *C. jejuni*, the lipooligosaccharide (LOS) is a main driver of virulence. We investigated the LOS structure of four *C. concisus* clinical isolates and correlated the inflammatory potential of each isolate with bacterial virulence. Mass spectrometric analyses of lipid A revealed a novel hexa-acylated diglucosamine moiety with two or three phosphoryl substituents. Molecular and fragment ion analysis indicated that the oligosaccharide portion of the LOS had only a single phosphate and lacked phosphoethanolamine and sialic acid substitution, which are hallmarks of the *C. jejuni* LOS. Consistent with our structural findings, *C. concisus* LOS and live bacteria induced less TNF-α secretion in human monocytes than did *C. jejuni*. Furthermore, the *C. concisus* bacteria were less virulent than *C. jejuni* in a *Galleria mellonella* infection model.[JLR] The correlation of the novel lipid A structure, decreased phosphorylation, and lack of sialylation along with reduced inflammatory potential and virulence support the significance of the LOS as a determinant in the relative pathogenicity of *C. concisus*.—Brunner, K., C. M. John, N. J. Phillips, D. G. Alber, M. R. Gemmell, R. Hansen, H. L. Nielsen, G. L. Hold, M. Bajaj-Elliott, and G. A. Jarvis. **Novel *Campylobacter concisus* lipooligosaccharide is a determinant of inflammatory potential and virulence.** *J. Lipid Res.* **2018.** 59: 1893–1905.

Supplementary key words cytokines • glycolipids • inflammation • lipid A • mass spectrometry • monocytes • phosphorylation • toll-like receptors

Campylobacter concisus is a member of the *Campylobacter* genus with as-yet-unclear pathogenic potential. Following the initial identification of *C. concisus* in patients with periodontal disease, recent investigations indicate this non-jejuni and -coli *Campylobacter* species has a role in acute and chronic human gastrointestinal (GI) conditions (1–5). This notion, however, remains a topic of debate because in general its overall high prevalence in patients and healthy

individuals alike suggests a commensal-like nature for *C. concisus* compared with *C. jejuni* (6, 7). Nonetheless, increased prevalence of *C. concisus* DNA in samples of patients with ulcerative colitis, pediatric Crohn's disease, gastroesophageal reflux, and Barrett's esophagus disease has been reported (5, 8–12). Furthermore, *C. concisus* and other non-*jejuni* and -*coli Campylobacter* species have been implicated as causal agents in prolonged mild endemic diarrhea in children and in traveler's diarrhea (11, 13, 14). Recent meta-analyses have also revealed an association of *Campylobacter spp.*, mainly *C. concisus* and *C. showae*, with an increased risk of inflammatory bowel disease (15).

C. concisus can attach to and invade intestinal epithelial cells and cause the secretion of proinflammatory cytokines, likely by a toll-like receptor 4 (TLR4)-dependent mechanism (9, 16). Adherence, invasion, and a proinflammatory phenotype may be strain-specific characteristics important in the pathogenesis of Proteobacteria such as *C. concisus* and some *Escherichia coli* (17). In general, bacterial lipopolysaccharide (LPS) and lipooligosaccharide (LOS) activate TLR4 and are important virulence factors for Gram-negative bacteria (18–21). In *C. jejuni,* the hydrophobic lipid A backbone of the LOS is hexa-acylated and is known to be a potent activator of TLR4 (22, 23). The interaction of LOS with TLR4 triggers a downstream signaling cascade by activating the NF-κB transcription factor and subsequent secretion of proinflammatory cytokines such as TNF-α and interleukin 8. Apart from TLR4 engagement, *C. jejuni* LOS also plays a role in bacterial invasion, colonization, and stress survival (23–25).

The biosynthesis region of *C. jejuni* LOS is highly variable between species possessing major differences in the content and organization of genes encoding LOS carbohydrate moieties and their linkages. In addition, the LOS gene locus is prone to frequent phase variations, resulting in broad structural heterogeneity among strains (26, 27). Major differences are observed in the outer region of the oligosaccharide (OS) moiety, but variations in lipid A phosphorylation and the number of amide linkages are also present (22). The lipid A disaccharide of *C. jejuni* comprises either 2-amino-2-deoxy-D-glucose (glucosamine; GlcN) or 2,3-diamino-2,3-dideoxy-D-glucose (GlcN3N); thus, the number of amide linkages to the acyl chains can vary from two (GlcN-GlcN) to four (GlcN3N-GlcN3N). Lipid A is hexa-acylated with either myristic (C14:O) or palmitic (C16:O) fatty acids, four of which are hydroxy fatty acids and are directly linked to the disaccharide residue (22, 28).

There is significant heterogeneity in the position and number of phosphate and phosphoethanolamine (PEA) residues bound to the OS and lipid A of the *C. jejuni* LOS (28). Amide linkages and lipid A phosphorylation have been shown to affect TLR4 activation (22, 29, 30). Although the core OS of *C. jejuni* is primarily conserved, significant variations in the outer OS region (31), which can contain *N*-acetylneuraminic acid (NeuAc, sialic acid) residues that are thought to modulate TLR4 activation, have been found (22, 32, 33).

Although there has been progress in the understanding of *C. jejuni* LOS and its role in the pathogenesis of human disease (22, 32, 34), the structure and heterogeneity of *C. concisus* LOS has remained unstudied. Such investigations could be informative regarding the relative pathogenicity and/or commensalism of *C. concisus* in humans. The aims of this study were to delineate the characteristics of the *C. concisus* LOS structure and inflammatory potential compared with the characteristics of *C. jejuni* LOS.

MATERIALS AND METHODS

Bacterial strains and LOS extraction

Clinical *C. concisus* isolates were isolated from the sigmoid colon biopsy of a newly presenting male pediatric patient diagnosed with Crohn's disease as part of the BISCUIT study (B38) (35) and from feces of patients with acute gastroenteritis (2010-131105, 2010-347972) (10, 11). The *C. concisus* NCTC 12408 strain is commercially available and originates from pediatric enteritis. *C. jejuni* 11168H is a variant of the human diarrhea isolate NCTC 11168 (36). The latter two strains were a kind gifts from David Guilliano (University of East London) and Brendan Wren (London School of Hygiene and Tropical Medicine), respectively. Bacterial strains were grown on blood agar no. 2 containing 0.5% yeast extract (Oxoid, Basingstoke, UK) and 5% defibrinated horse blood (Sigma-Aldrich, Gillingham, UK). All strains were grown at 37°C in a gas jar under microaerobic conditions generated by using a CampyGen sachet (Oxoid). For *C. concisus* strains the microaerobic atmosphere was supplemented with $\sim$10% H_2 generated with sodium borohydride (Sigma-Aldrich) (37). *C. jejuni* and *C. concisus* strains were grown for 24 and 72 h, respectively, harvested, and stored at $-80°C$ prior to use. Bacterial LOS was extracted and purified by a modification of the hot phenol-water method as described previously (22).

SDS-PAGE analysis

LOS samples of 10 μg were subjected to SDS-PAGE using a 12% polyacrylamide gel (PROTEAN II xi cell; Bio-Rad, Hercules, CA) in Tris-glycine running buffer. The gel was fixed for 1 h in 40% methanol and 5% acetic acid, and LOS was visualized by silver staining (38).

Preparation of intact LOS for MALDI-TOF MS

LOS samples were prepared for MS analysis as previously described (18). Briefly, purified LOS (10 mg/ml) was suspended in a methanol-water (1:3) solution containing 5 mM EDTA. An aliquot was desalted with cation exchange beads (Dowex 50WX8-200). The desalted sample solution was mixed with 100 mM dibasic ammonium citrate (9:1 v/v), and 1–2 μl was spotted onto a thin layer of matrix composed of a 4:1 solution of 2,4,6-trihydroxyacetophenone (200 mg/ml in methanol; Sigma-Aldrich) with nitrocellulose (15 mg/ml in acetone-isopropanol [1:1]; Bio-Rad). Samples were left to air dry prior to analysis.

O-deacylation of LOS

Native LOS ($\sim$300 μg) was incubated with 200 μl anhydrous hydrazine (Sigma-Aldrich) at 37°C for 2 h with intermittent vortexing. The reaction was stopped with 1 ml precooled acetone ($-20°C$), and the *O*-deacylated LOS samples were pelleted by centrifugation at 10,000 *g*, washed with chilled acetone, centrifuged again, dissolved in 20 μl water, lyophilized, and stored at $-80°C$.

HF treatment of LOS

Phosphoesters were partially removed by hydrogen fluoride (HF) treatment. Native LOS (10 mg/ml) was reacted with 48%

aqueous HF at 4°C for 16–20 h. Excess HF was removed using a Savant SpeedVac (Thermo Fisher Scientific, Waltham, MA) with an in-line trap.

High-resolution MALDI-TOF and IMS-MS

MALDI-TOF MS and ion-mobility spectrometry (IMS)-MS analyses were performed on a Synapt G2 high-definition MS system (Waters Corporation, Milford, MA) in sensitivity mode. The instrument is equipped with a T-wave ion-mobility cell (Triwave[TM]) (39, 40) and was operated in MALDI mode as previously described (41). Spectra were obtained in negative- or positive-ion mode operating a neodymium-doped yttrium aluminum garnet laser at 355 nm and 200 Hz. In general, spectra were acquired for ∼1–2 min with a scan duration of 1.0 s and an overall cycle time of 1.024 s. The instrument was calibrated using the masses of the monoisotopic ions for porcine renin substrate, intact bovine insulin, and B chain.

The T-wave device on the Synapt G2 high-definition MS system consists of three cells: a trap cell, IMS cell, and transfer cell. For IMS-MS experiments, the T-wave peak height voltage was 40 V, and the T-wave velocity used was generally a variable wave velocity of 650 to 250 m/s. Typically, the T-wave mobility cell contained nitrogen at a pressure of ∼2 mbar. The trap gas flow was 0.4 ml/min, the helium cell gas flow was 180 ml/min, and the IMS gas flow was 90 ml/min. The trap DC bias was 80 V.

MS/MS with IMS was performed typically by selecting precursor ions with instrument LM and HM resolution settings of 4.7 and 15.0, respectively. In initial TOF MS/MS mode without IMS, fragmentation was achieved by applying collision energy with argon as the collision gas in the trap region of the T-wave ion-mobility cell. Collision energies of 85–110 V were required for optimum fragmentation of intact LOS or prompt fragment ions (pseudo-MS^3) in the trap. For IMS-MS/MS experiments, collision energy was also applied with argon as the collision gas in the transfer cell after IMS separation at values ranging from 50 to 90 V, depending on the analyte. For the analysis of OS and lipid A prompt fragments, a T-wave variable wave velocity of 1,100 to 200 m/s was used. 2D IMS spectra were viewed using DriftScope 2.1 software, and selected spectral regions were exported to MassLynx with retention of drift-time information for the generation of mobilograms and subspectra. Chemical structures were generated using the ChemBioDraw Ultra software.

Genomic analysis

Genomic analysis of the *C. concisus* strains used in our study was carried out to look for the presence or absence of genes involved in PEA transfer and in sialic acid biosynthesis and transfer. The genomes of three of the strains (B38, 2010-131105, and 2010-347972) and 53 additional *C. concisus* strains were recently whole genome sequenced, and the genomes were assembled (42). In addition, the following analyses were carried out on 36 other publicly available *C. concisus* strains (2, 43–47).

Gene and protein prediction of genome assemblies was carried out with Prokka (48). The Prokka dependencies BioPerl (49), GNU parallel (50), BLAST+ (51), and Prodigal (52) were utilized along with the recommended and optional tools Aragorn (53), Barrnap (https://github.com/Victorian-Bioinformatics-Consortium/barrnap) (42), HMMER3 (54), Infernal (55), RNAmmer (56), and SignalP (57). Annotation of predicted genes and proteins was carried out with BlastKOALA (58).

PCR validation of LOS genes

PCR validation of the genome analysis was performed using the primer pair *eptC*-F (CCAGATGAAGCCGGTGAGTT) and *eptC*-R (T[G/A]CTCCAAGGCT[C/T]TTTGCTT), which amplifies a 578 bp region of the PEA transferase gene *eptC*, and the primer pair *waaC*-F (TGGCT[A/C]GTTGATGCCCGTTT) and *waaC*-R

(ATCGCCTCAGCTCTTGC[T/C]TT), which amplifies a 522 bp region of the LOS heptosyl transferase I *waaC* gene, which is the first within the LOS gene cluster. PCR conditions were as follows: *eptC*: 94°C for 5 min, 30 cycles of 94°C for 30 s, 57°C for 30 s, and 72°C for 30 s, followed by 72°C for 10 min; *waaC*: 94°C for 5 min, 30 cycles of 94°C for 30 s, 50°C for 30 s, and 72°C for 30 s, followed by 72°C for 10 min.

TNF-α secretion by THP-1 monocytic cells and PBMCs

The human monocytic cell line THP-1 was obtained from the American Type Culture Collection (Manassas, VA) and propagated in RPMI 1640 supplemented with 10% FBS at 37°C in a 5% CO_2 atmosphere. The cells were differentiated with 10 ng/ml PMA (Sigma-Aldrich) for 18 h as previously reported (59). The differentiated THP-1 cells were seeded at 1.2×10^5 cells per well in 96-well plates and treated with 100 ng/ml LOS or culture media only for 18 h. The supernatants were collected and stored at −80°C until analysis.

Peripheral blood mononuclear cells (PBMCs) were isolated from venous blood obtained from seven healthy adult volunteers following the manufacturer's protocol (Lymphoprep[TM]; Axis-Shield, Dundee, UK). PBMCs (2×10^6 cells/ml) were suspended in RPMI 1640 medium with 10% FBS and cocultured with bacteria (multiplicity of infection = 100), and supernatants were collected after 18 h. TNF-α cytokine release was determined using a Ready-Set-Go TNF-α ELISA kit (Affymetrix, San Diego, CA) following the manufacturer's instructions.

Blood samples were obtained with informed consent and ethical approval from the Institute of Child Health/Great Ormond Street Hospital Research Ethics Committee and in accordance with the Declaration of Helsinki.

Galleria mellonella infection model

G. mellonella larvae (UK Waxworms Ltd., Dinnington, UK) were injected into the second foreleg with a bacterial suspension in 10 μl inocula ($n = 15$; ∼10^7 CFU) (60, 61). Larvae were incubated at 37°C, and survival was monitored at 24 h intervals for 5 days. PBS injection served as a control.

Statistical analysis

One-way ANOVA with Tukey posttest was applied for multiple comparison analysis. Survival curves were analyzed by the Mantel-Cox log-rank test. GraphPad Prism 7.00 software was used for analysis.

RESULTS

Heterogeneity between *C. concisus* LOS structures

To investigate the structure of *C. concisus* LOS, we first analyzed intact LOS that was isolated from four *C. concisus* GI strains by MS and SDS-PAGE. LOS was also extracted from the *C. jejuni* 11168H strain and used for comparison. Spectra of the intact LOS were obtained in high-resolution reflectron-mode negative-ion MALDI-TOF MS that enabled measuring monoisotopic molecular ions with high mass accuracy (<35 ppm). The spectra provided evidence of varied and multiple LOS molecular ions, with some ions detected above *m/z* 5,000 in all four *C. concisus* LOS samples (**Fig. 1A–D**). Peaks for the molecular ions of the *C. jejuni* 11168H LOS were of lower mass in the range of *m/z* 3,600 to 4,300 (Fig. 1E). This is in agreement with previous MS studies of intact *C. jejuni* LOS from other strains that
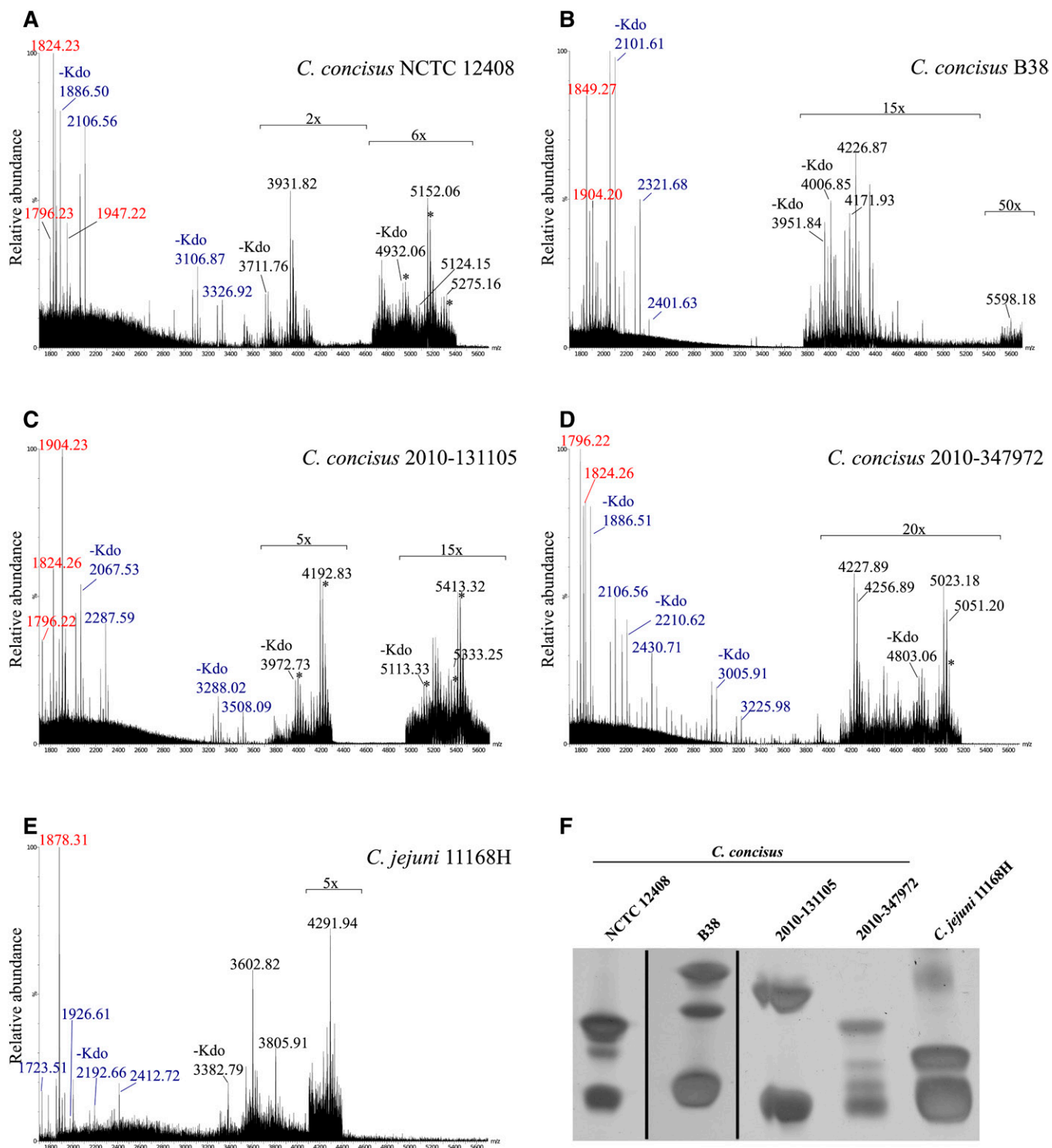
Fig. 1. Negative-ion MALDI-TOF spectra and LOS profiles of *C. concisus* and *C. jejuni* LOS. A–E: Negative-ion MALDI-TOF MS spectra for the LOS of *C. concisus* isolates NCTC 12408, B38, 2010-131105, 2010-347972, and *C. jejuni* 11168H, respectively. The relative abundance of the peaks was magnified where indicated. The *m/z* values presented are for the monoisotopic peaks observed (red font for lipid A fragments, blue font for OS fragment ions, and black font for molecular ions). Asterisks show peaks corresponding to sodiated molecular or fragment ion peaks. Purified LOS (10 μg per lane) of *C. concisus* isolates NCTC 12408, B38, 2010-131105, 2010-347972, and *C. jejuni* 11168H were separated by SDS-PAGE and stained using silver nitrate. F: The gel was cropped where indicated (black lines).

reported molecular ion peaks of lower mass than those for the LOS of the *C. concisus* isolates (22, 62, 63).

The SDS-PAGE profile of the *Campylobacter* LOS showed the presence of multiple bands in all samples (Fig. 1F),

which was consistent with the heterogeneity in the LOS that was revealed by the MS analyses. In accordance with the MALDI-TOF MS data, the electrophoretic mobility of the slow migrating bands was indicative of larger LOS moieties

in the *C. concisus* isolates compared with the *C. jejuni* LOS. The *C. concisus* isolates with bands for the largest LOS moieties were B38 and 2010-131105, and these appear to be in agreement with the molecular ion peaks observed in the negative-ion spectra at *m/z* 5,598.18 (Fig. 1B) and *m/z* 5,413.32 (Fig. 1C), respectively.

Prompt fragmentation of the labile 2-keto-3-deoxyoctulosonic acid (Kdo)-lipid A bond of the LOS occurring in the MALDI source produced abundant lipid A and OS fragment ions of the LOS. Observed peaks corresponding to the loss of Kdo (220.06 Da) aided in the identification of peaks for OS fragment ions and LOS molecular ions. An attribute of this methodology is that abundant lipid A and OS fragment ions are produced together with molecular ions for the intact LOS that thus enables more certain identification of the latter and provides an opportunity to obtain top-down sequence information. For example, the observed peak at *m/z* 1,904.23 for the monoisotopic mass of the largest lipid A fragment ion of *C. concisus* isolate 2010-131105 LOS (Fig. 1C) together with that for the OS fragment ion at *m/z* 2,287.59 plus a proton gives a value of *m/z* 4,192.83, corresponding to the monoisotopic mass of the prominent molecular ion peak for intact LOS.

IMS MALDI-TOF MS was used to separate intact LOS and the prompt lipid A and OS fragment ions formed in the source (**Fig. 2**). Due to the differences in the shape and size of the lipid A and OS fragments and intact LOS, the ions were separated by IMS to provide more evidence of distinct molecular characteristics. In some cases, the ion types occurred in otherwise overlapping regions of the spectra. The IMS enabled the extraction of subspectra of specific ion types, permitting unambiguous classification of ions and mass measurements. The spectra of the LOS from each isolate contained unique OS fragment ions and molecular ions for intact LOS but contained some similar peaks for lipid A fragment ions (**Table 1**).

MS/MS analysis of the lipid A moiety

We performed negative-ion MS/MS analysis with IMS to obtain sequence information and structural details regarding the lipid A and OS moieties (supplemental Fig. S1). Differences in the IMS drift time of the lipid A fragment ions compared with ions for OS fragments or non-LOS species of similar *m/z* values resulted in cleaner MS/MS spectra and enabled more confident interpretations of the MS/MS spectra. This is illustrated by the MS/MS spectrum of the lipid A fragment ions at *m/z* 1,824.3 (supplemental Fig. S1B, top) from *C. concisus* LOS strain 2010-131105. Without IMS, we would have detected some of the less abundant but significant non-lipid A fragment ions deriving from the peak at *m/z* 1,821.60 shown in the MS/MS spectrum (supplemental Fig. S1B, bottom).

Hydrazine treatment of LOS was performed to hydrolyze the *O*-linked acyl chains from the lipid A while the *N*-linked fatty acyl groups remained intact. An IMS-MS/MS negative-ion spectrum (**Fig. 3A**, C) was obtained of the *O*-deacylated lipid A fragment ion (*m/z* 979.5) from the LOS of *C. concisus* strain 2010-131105. The fragment ion peaks observed were in accordance with the presence of a disaccharide containing two GlcN residues with β-hydroxy myristic acid (C14:0[3-OH]) and β-hydroxy palmitic acid (C16:0[3-OH]) linked to the amino groups on the nonreducing and reducing terminal monosaccharide residues, respectively. Peaks corresponding to B- and Y-type fragment ions as well as cross-ring fragment ions (^{0,2}A and ^{0,4}A) provided evidence for two different lipid A structures (Fig. 3A), one with phosphate on both ends (bisphosphorylated) and one diphosphorylated lipid A with a single pyrophosphoryl group (supplemental Table S1).

Negative-ion IMS-MS/MS of the *m/z* 1,824.3 ions for the intact lipid A of strain 2010-131105 produced fragment ion peaks at *m/z* 1,726.33 corresponding to the loss of H_3PO_4 (−97.98 Da) at *m/z* 1,580.10, consistent with the loss of C14:0(3-OH) (−244.20 Da), and at *m/z* 1281.96, consistent with sequential losses of H_3PO_4, C14:0(3-OH), and C12:0 (−200.18 Da). The ^{0,4}A-type cross-ring B- and Y-type fragment ions detected in the MS/MS spectrum of the intact lipid A also were in agreement with the expression of di- and bisphosphorylated hexa-acylated lipid A (Fig. 3B, D), confirming our interpretation of the MS/MS spectrum of the *O*-deacylated lipid A. In addition, low-mass fragment ions were observed in the negative-ion MS/MS spectra at *m/z* 158.9 for $HP_2O_6^-$, providing further support for the presence of pyrophosphoryl groups on the diphosphorylated lipid A.

In total, we identified five different lipid A moieties in *C. concisus* LOS (**Table 2**). All were in accordance with a disaccharide of two GlcN residues that contained a total of two amide linkages. Fragment ions at *m/z* 1,824.2 or higher corresponded to the same fatty acid profile as the lower-mass fragment ions at *m/z* 1,796.2, but with an exchange of a C16:0(3-OH) residue for a C14:0(3-OH). An additional phosphate or PEA moiety accounted for all of the other high-mass lipid A species observed in the spectra of the *C. concisus* isolates (Table 2).

Overall, the data showed that the hexa-acylated *C. concisus* LOS has some similarity to *C. jejuni* LOS; however, clear differences were identified (**Fig. 4**). Both contain four hydroxy fatty acids, but there is a single C16:0(3-OH) in most *C. concisus* lipid A moieties, in place of one of the C14:0(3-OH) moieties on *C. jejuni* LOS. There are two secondary fatty acids on the nonreducing terminal glucosamine in lipid A of both species, but these were identified as C14:0 and C12:0 in *C. concisus*, in contrast to the two C16:0 acyl chains on the nonreducing terminal glucosamine of *C. jejuni* lipid A (28, 64).

Analyses of the OS moieties

Although the lipid A moieties of the *C. concisus* strains possessed significant similarities, we identified peaks of unique masses corresponding to OS fragment ions in the spectra of the LOS of each isolate (Fig. 1, Table 1). HF treatment of the LOS was used to remove and aid in establishing the presence of phosphoesters. A comparison of positive-ion MALDI-TOF MS spectra of the HF-treated and untreated LOS of *C. concisus* NCTC 12408 confirmed that there was a single phosphate substituent (HPO₃; 79.97 Da) as part of the inner-core OS observed at *m/z* 2,108.6 in untreated LOS (supplemental Fig. S2).

A

B
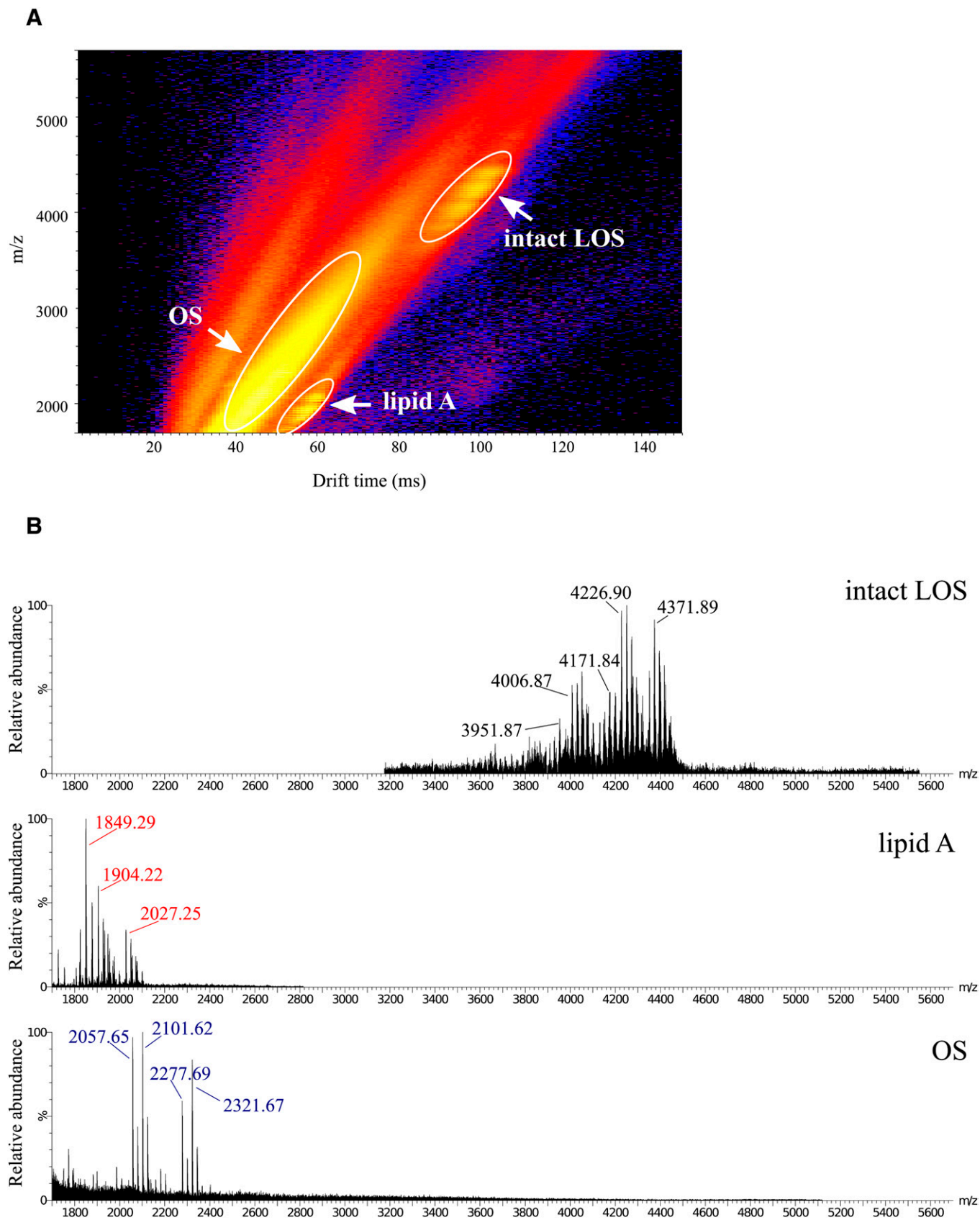
Fig. 2. Analysis of intact LOS from *C. concisus* B38 by MALDI-TOF MS with IMS. The panel shows a 2D plot of the IMS data set. A: Differences in drift time allow for the separation of low-molecular-weight components of non-LOS origin, OS prompt fragment ions, intact LOS, and lipid A prompt fragment ions. B: Regions of the mass spectra of the $(M\text{-}H)^-$ molecular ions, lipid A prompt fragments, and OS prompt fragments. Spectra were acquired with the Synapt G2 high-definition mass spectrometer using IMS and analyzed with DriftScope and MassLynx software.

TABLE 1. Observed $(M-H)^-$ peaks for lipid A and OS fragment ions and corresponding intact LOS

Strain	Lipid A	OS	Intact LOS
C. concisus NCTC 12408	1,796.23	3,326.92	5,124.15
	1,824.23	3,326.92	5,152.06
	1,947.22	3,326.92	5,275.16
C. concisus B38	1,849.27	2,321.68	4,171.93
	1,904.20	2,321.68	4,226.87
			5,598.18
C. concisus 2010-131105	1,904.23	2,287.59	4,192.83
	1,824.26	3,508.09	5,333.25
	1,904.23	3,508.09	5,413.32
C. concisus 2010-347972	1,796.22	2,430.71	4,227.89
	1,796.22	3,225.98	5,023.18
	1,824.26	3,225.98	5,051.20
C. jejuni 11168H	1,878.31	1,723.51	3,602.82
	1,878.31	1,926.61	3,805.91
	1,878.31	2,412.72	4,291.94

The presence of a single phosphate in the core OS was further established by MALDI-TOF IMS MS/MS analyses in the positive-ion mode of the untreated and HF-treated NCTC 12408 LOS. Extensive fragmentation produced losses in accordance with the presence of expected monosaccharide components such as Kdo, heptose (192.06 Da), hexose (162.05 Da), and hexosamine (HexN; 161.07 Da) (supplemental Fig. S3). A loss of 175 Da, possibly corresponding to hexosaminuronic acid (HexNA; 175.05 Da) was detected in some of the spectra and apparently corresponded to low-mass
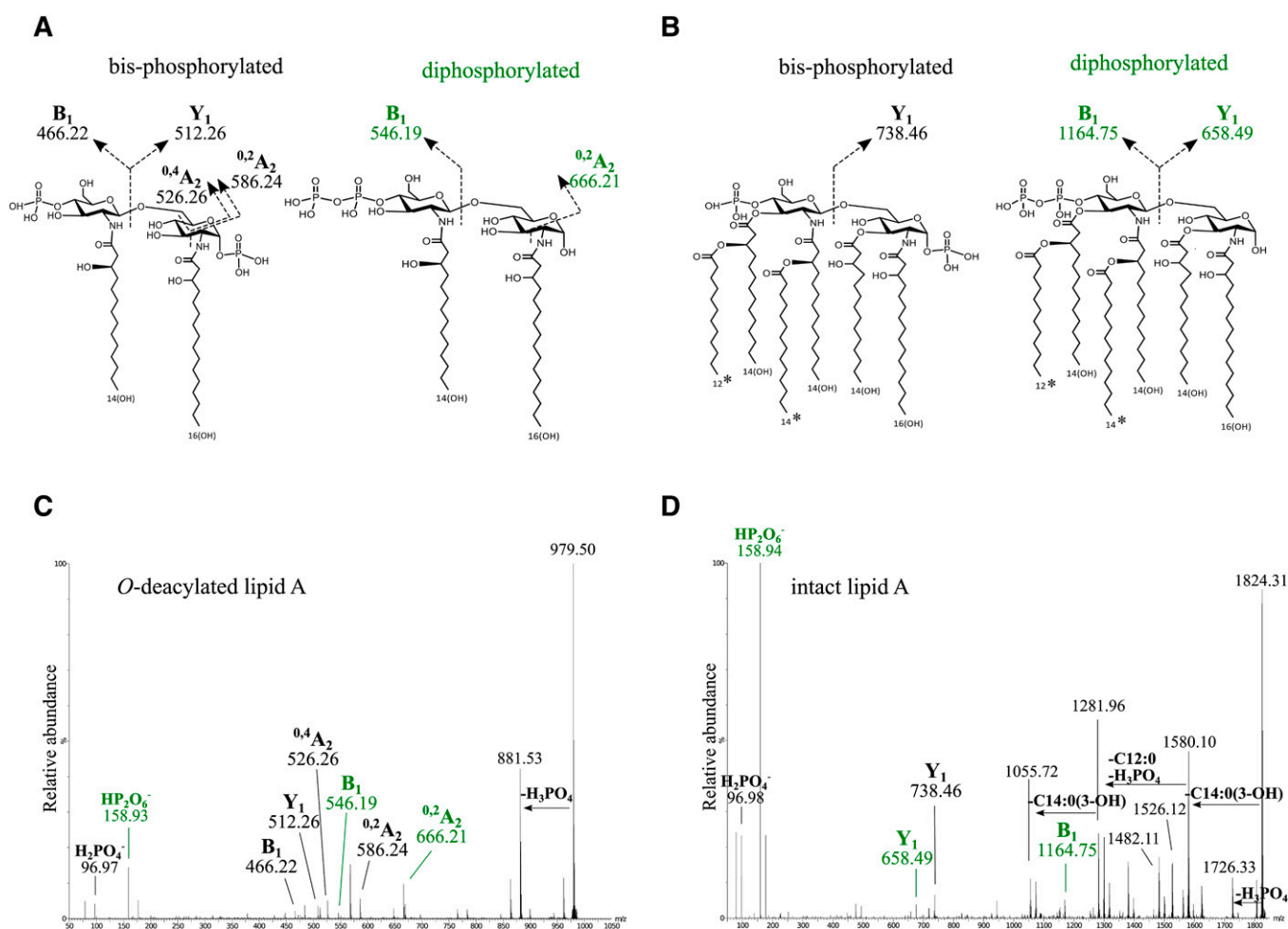
Fig. 3. Negative-ion IMS-MS/MS spectra of *O*-deacylated and intact lipid A of *C. concisus* 2010-131105. A, C: Proposed structure and fragmentation from MS/MS of *O*-deacylated lipid A of *C. concisus* 2010-131105. B, D: Proposed structure and fragmentation from MS/MS of intact lipid A of *C. concisus* 2010-131105. Fragment ion peaks observed in the MS/MS spectrum of the parent ions at *m/z* 979.50 of the *O*-deacylated (C) and parent ions at *m/z* 1,824.31 in the intact lipid A (D) were consistent with B-, Y-, ^{0,4}A-, and ^{0,2}A-type fragment ions as indicated in the proposed structures. The asterisk indicates potential interchange in the positions of two fatty acids. The green-colored labels are for fragment ions consistent with a lipid A with a single pyrophosphoryl group.

TABLE 2. Proposed compositions and observed and calculated negative Y-ion type peaks for lipid A fragment ions of intact *C. concisus* LOS

Composition	HexN-HexN	HexN-HexN	HexN-HexN	HexN-HexN	HexN-HexN
	4 C14:0(3-OH)	3 C14:0(3-OH) C16:0(3-OH)	3 C14:0(3-OH) C16:0(3-OH)	3 C14:0(3-OH) C16:0(3-OH)	3 C14:0(3-OH) C16:0(3-OH)
		C14:0	C14:0	C14:0	C14:0
		C12:0	C12:0	C12:0	C12:0
	2P	2P	2P PEA(-H$_3$PO$_4$)	3P	2P PEA
Calculated *m/z*	1,796.21	1,824.24	1,849.27	1,904.21	1,947.25
			Observed *m/z* (Δppm)		
NCTC 12408	1,796.23 (10.3)	1,824.23 (−7.1)			1,947.22 (−16.1)
B38			1,849.27 (−2.4)	1,904.20 (−4.8)	
2010-131105	1,796.22 (4.7)	1,824.26 (9.4)		1,904.23 (10.9)	
2010-347972	1,796.22 (4.7)	1,824.26 (9.4)			

fragment ion peaks observed in positive-ion spectra at *m/z* 176.06, as observed in supplemental Fig. S3.

Elements of commonality were detected in the spectra of the LOS from *C. concisus*. Monoisotopic OS fragment ions were observed at *m/z* 2,106.56 in the negative-ion spectra of intact LOS from both NCTC 12408 and 2010-347972 (Fig. 1A, D), presumably for the core OS. In addition, there was a neutral loss of 1,220.4 Da from both LOS molecular ion and OS fragment ions in spectra of NCTC 12408 (OS peaks at *m/z* 3,326.92 and 2,106.56) and 2010-131105 (OS peaks at *m/z* 3,508.09 and *m/z* 2,287.59; Fig. 1A, C). The OS structures could be related to the semi-rough-type LPS observed in some Gram-negative bacteria that contain one *O*-antigen repeat unit (65).

Lack of nonreducing terminal sialic acid (NeuAc) on the *C. concisus* LOS was established by negative-ion MS/MS of molecular ions of intact LOS (**Fig. 5**). Collisional activation of the molecular ions of the intact LOS from the four strains of *C. concisus* (Fig. 5A–D) produced abundant fragment ions for the loss of Kdo (220.06 Da), followed by the loss of HPO$_3$ and H$_2$PO$_4$ (97.98 Da). For example, MS/MS

of (M-H)$^-$ of intact LOS from NCTC 12408 at *m/z* 5,152.10 produced a prominent peak at *m/z* 4,932.02 for the loss of Kdo (Fig. 5A). Similarly, collisional activation of the (M-H)$^-$ ions at *m/z* 4,226.87 for intact LOS from strain B38 produced a prominent peak at *m/z* 4,006.82 corresponding to a loss of Kdo and a peak at *m/z* 3,926.82 for the loss of both Kdo and HPO$_3$ (Fig. 5B). Peaks for similar fragments of the LOS molecular ion were also observed for the other two *C. concisus* strains (Fig. 5C, D).

In contrast, the MS/MS spectra of molecular ions of the intact LOS from *C. jejuni* (Fig. 5E, F) contained fragment ion peaks consistent with the loss of Kdo as well as the loss of both Kdo and NeuAc (291.10 Da). For example, collisional activation of the (M-H)$^-$ ions at *m/z* 4,292.08 (Fig. 5E) from the *C. jejuni* LOS produced abundant fragment ions at *m/z* 4,072.00 for the loss of Kdo and a peak at *m/z* 3,780.93 for the loss of Kdo and NeuAc. Fragment ions from the loss of NeuAc are consistent with nonreducing terminal sialylation that have previously been established as being present on the 11168H LOS (22). However, corresponding fragment ion peaks for the loss of NeuAc were
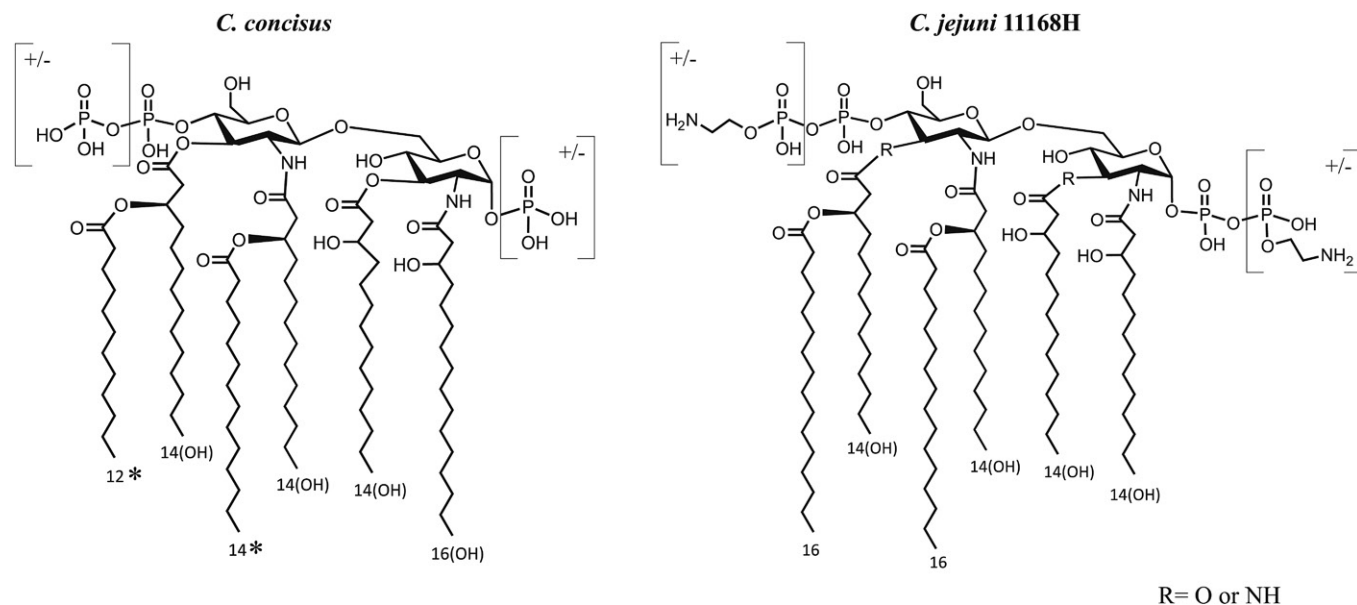

Fig. 4. Schematic of consensus structures of *C. concisus* and *C. jejuni* 11168H lipid A. The asterisk indicates potential interchange in the positions of two fatty acids.
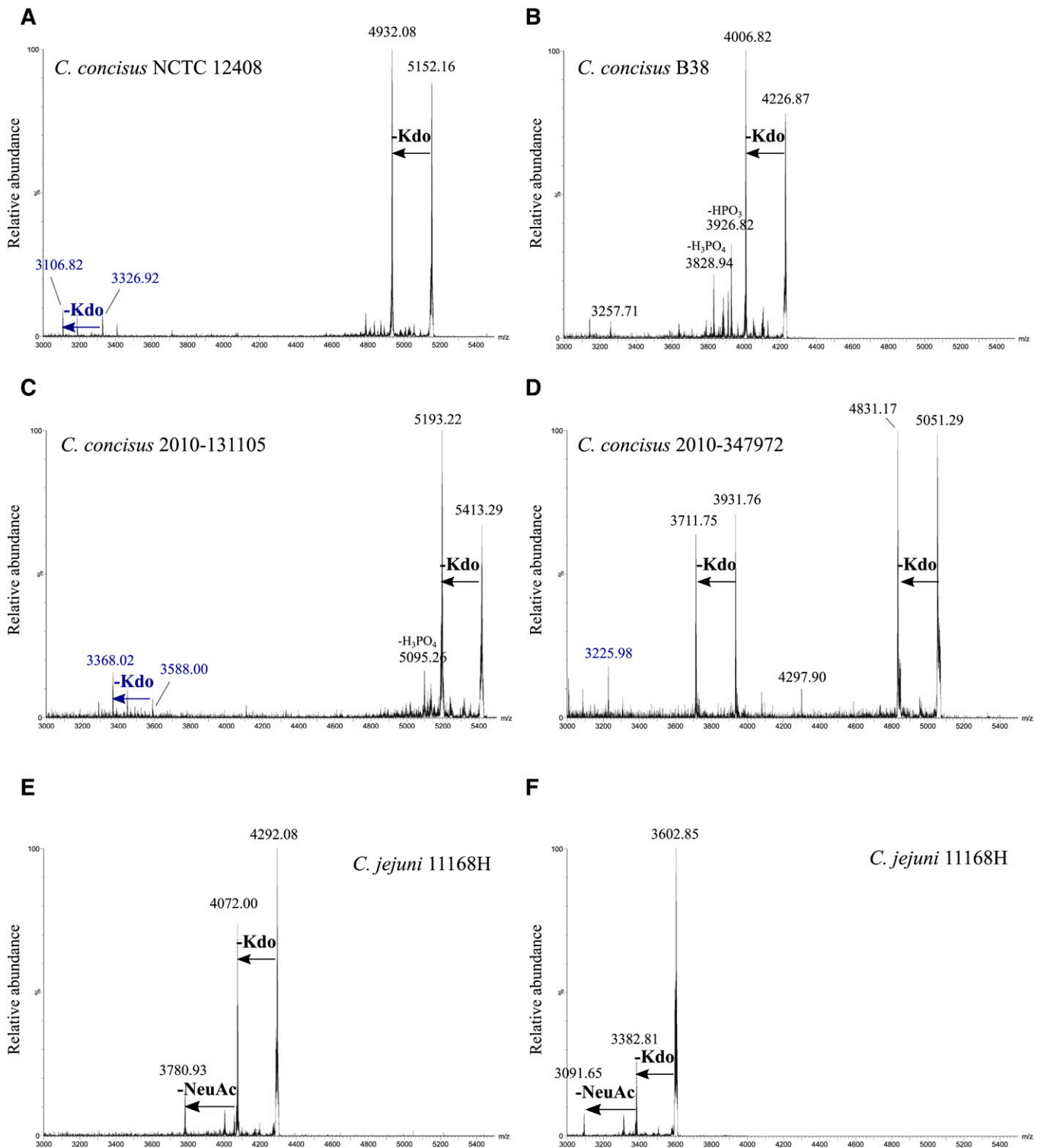
Fig. 5. Negative-ion MALDI-TOF MS/MS analysis of intact LOS ions. A–D: Negative-ion MALDI-TOF MS/MS spectra for an LOS molecular ion (M-H)⁻ peak of each *C. concisus* isolates NCTC 12408, B38, 2010-131105, and 2010-347972. E, F: Negative-ion MALDI-TOF MS/MS spectra for two intact LOS ions of *C. jejuni* 11168H. The mass of the losses observed are consistent with the fragments of known carbohydrate or phosphoryl moieties as indicated. Labels in blue font indicate fragment ions corresponding with OS fragments as previously observed.

strikingly absent in the MS/MS of intact LOS from the 4 *C. concisus* strains.

Genomic analyses of LOS biosynthetic genes

We conducted a genomic analysis of three *C. concisus* strains to look for the presence or absence of genes involved in PEA transfer and in sialic acid biosynthesis and transfer. We looked specifically for the presence of sialic acid synthase (*neuB1*), sialic acid transferase (*cstII*), PEA transferase (*eptC*), and heptosyl transferase (*waaC*), which is known to be the first gene within the LOS gene cluster (66). An analysis of whole genome sequences indicated

that all three strains contained *waaC*, whereas none of the strains contained *neuB1* or *cstII*, confirming the lack of sialic acid synthesis machinery. The presence of *waaC* was further confirmed by PCR analysis. This lack of sialic acid synthesis capability was also confirmed in all 89 published *C. concisus* genomes. When we looked for the presence of the PEA transferase *eptC* gene within all of the *C. concisus* genomes, we found that most strains (69%) did not contain the *eptC* gene; however, all three of the strains used in this study were *eptC*-positive, which was also confirmed by PCR analysis.

Inflammatory and virulence potential of *C. concisus* isolates

The LOS-induced TLR4 signaling cascade is crucial in triggering monocytic innate immune responses to *C. jejuni* that result in TNF-α secretion (22). To determine the proinflammatory potential of *C. concisus* LOS, differentiated THP-1 monocytes were treated with purified LOS from all four *C. concisus* strains and from the *C. jejuni* 11168H strain for 18 h prior to quantification of the proinflammatory cytokine TNF-α. Notably, the LOS from all *C. concisus* strains elicited a significantly reduced TNF-α response compared with the *C. jejuni* 11168H LOS (**Fig. 6A**; $P < 0.001$). To confirm the importance of LOS signaling in this context, PBMCs from seven healthy donors were cocultured with live bacteria of each of the four *C. concisus* strains and *C. jejuni*. As seen in the response to purified LOS, the *C. concisus* live bacteria also induced significantly less TNF-α compared with *C. jejuni* 11168H (Fig. 6B; $P < 0.05$).

To assess bacterial virulence, we used a *G. mellonella* infection model. Larvae were infected with *C. concisus* isolates and *C. jejuni* 11168H, and survival was monitored over 5 days. *C. concisus* isolates were significantly less virulent (>85% *G. mellonella* survival) compared with *C. jejuni* (36% survival) (Fig. 6C; $P < 0.001$). Thus, our findings show that the *C. concisus* is less inflammatory and less virulent compared with *C. jejuni* and, furthermore, that these differences are reflected by the reduced inflammatory potential of the *C. concisus* LOS compared with the LOS of *C. jejuni*.

DISCUSSION

C. concisus is being increasingly found in the human GI tract, yet the contribution of this organism to homeostasis in health or to disease states is unclear. In this study, we aimed at defining and correlating the structure of *C. concisus* LOS with its bioactivity. Four clinical isolates were chosen from adult and pediatric patients presenting with gastroenteritis and Crohn's disease. The intact LOS of all four *C. concisus* isolates was larger than that of *C. jejuni*, which was primarily due to the differential size of the OS moiety. In addition, significant heterogeneity between the OS of the *C. concisus* isolates was observed. Heterogeneity in the *C. jejuni* LOS, particularly in the outer region of the OS, has been previously described and was ascribed to differences in the
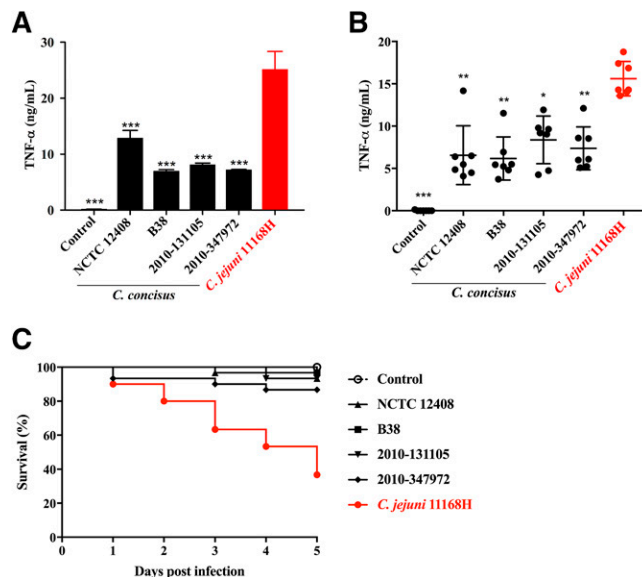

Fig. 6. Inflammatory potential and virulence of *C. concisus* isolates. A: Differentiated THP-1 cells were stimulated with purified (100 ng/ml) LOS for 18 h prior to the quantification of TNF-α secretion by ELISA. Results are expressed as the mean ± SD of eight biological replicates. Stars indicate statistical significant differences compared with *C. jejuni* as analyzed by ANOVA with Tukey post hoc test. B: Human PBMCs ($n = 7$) were cocultured with live bacteria at MOI 100 for 18 h prior to the quantification of TNF-α secretion by ELISA. Results are expressed as the mean ± SD of three independent experiments. Stars indicate statistical significant differences compared with *C. jejuni* as analyzed by ANOVA with a Tukey post hoc test (A, B). C: Survival of *G. mellonella* larvae exposed to *C. concisus* isolates and *C jejuni* 11168H. *G. mellonella* larvae were injected with a bacterial suspension (∼10^7 CFU), and their survival was monitored over time. Results represent the mean survival rate ($n = 30$) pooled from two independent experiments. Survival rates in the *C. jejuni* group were compared with each of the *C. concisus* groups ($P < 0.001$). The Mantel-Cox log-rank test was applied for statistical analysis. *$P < 0.05$; **$P < 0.01$; and ***$P < 0.001$.

gene content and frequent phase variations in the LOS gene loci (26). Variations primarily were observed in the outer region of the OS, whereas core OS and the general structure of the lipid A were found to be predominantly conserved (31). In line with these findings, we observed structural similarities in the lipid A and in likely monosaccharide components of the core OS in all four *C. concisus* isolates, whereas there appeared to be greater variability in the outer OS regions.

Hexa-acylation has been found to be a requisite for optimal engagement with TLR4 and its downstream signaling cascade (22). Despite the presence of a hexa-acylated lipid A moiety in the LOS of both *C. concisus* and *C. jejuni*, we observed less induction of TNF-α by PBMCs in response to *C. concisus* strains compared with *C. jejuni*. This may be due to the recognized relationship between the 3D shape of lipid A and its bioactivity. Specifically, it has been found that lipid A molecules with a more conical wedge-shaped conformation and a hydrophilic backbone that is smaller compared with that of the hydrophobic portion of the molecule as found in *C. jejuni* induce more inflammatory signaling compared with molecules with a

more cylindrical shape, as would be expected for the *C. concisus* lipid A due to the lack of secondary C16 acyl groups (67). Moreover, although *C. jejuni* strains can have up to two GlcN3N moieties in the lipid A, our data showed that the lipid A of the four *C. concisus* isolates contained no GlcN3N moieties, which is thought to affect the recognition of lipid A by the TLR4-MD2 complex due to differences in the flexibility of amide- versus ester-linked acyl chains (22, 30).

Apart from the nature of the acylation of the lipid A, other LOS/LPS modifications have been found to influence engagement with TLR4 and inflammatory signaling (20). Based on an analysis of a panel of livestock and non-livestock-associated *C. jejuni* isolates, we previously reported that increased numbers of phosphoryl substituents on the lipid A and the presence of sialic acid in OS contributed to TLR4-mediated inflammatory signaling by THP-1 cells and primary human monocytes, as reflected by TNF-α secretion (22).

C. jejuni produces LOS containing a core OS but lacking the repeating *O*-antigens, although *C. jejuni* LPS has been described (68, 69). Indeed, as reported by Karlyshev et al. (70), all *C. jejuni* strains express LOS, whereas the LPS structure observed in some strains appears to be genetically and structurally unrelated and bears closer resemblance to capsular polysaccharides. LOS of *C. jejuni* is heavily phosphorylated, containing one or two phosphates and up to three PEA groups on the lipid A and in many strains a PEA on the OS moiety (22). The presence of PEA on the cell surface of *C. jejuni* is associated with bacterial virulence by various mechanisms. Two recent studies identified the *eptC* gene encoding a novel transferase conferring PEA expression on flagellar rod proteins, *N*-linked glycans, and lipid A (71, 72). The addition of PEA to lipid A and the Hep on the core of the OS results in enhanced recognition of TLR4 and resistance to antimicrobial peptides and facilitates the ability of *C. jejuni* to colonize and survive in avian and murine hosts (29). Variations in PEA and the pyrophosphorylation of lipid A also have been shown to play an important role in TLR4 signaling by the pathogenic species *Neisseria meningitidis* and *N. gonorrheae*, whereas PEA and pyrophosphate are absent in the lipid A moiety of most commensal *Neisseria* strains that rarely cause disease and exhibit lower inflammatory potential (18, 73).

In our analyses of the *C. concisus* LOS, we found no evidence for PEA in the OS moiety but did detect an 80 Da difference corresponding to phosphate as part of the core of the OS moiety. Overall, most prominent lipid A peaks were consistent with non-PEA containing lipid A, although spectra of the intact LOS from two *C. concisus* isolates, NCTC 12408 and B38, contained a major peak for a lipid A moiety containing PEA. Interestingly, *eptC* genes were encoded in all three *C. concisus* strains subjected to whole genome sequencing, and this was further confirmed by PCR analysis. Despite this, two of the isolates did not express a major peak for PEA containing lipid A, suggesting that PEA expression may undergo genetic regulation. Altogether, no more than three phosphoryl substituents (including both phosphate and PEA) were detected on any of the *C. concisus* lipid A moieties. In contrast, our previous MS analyses of the *C. jejuni* LOS revealed that the lipid A contained a total of two to five phosphoryl-containing groups (22). Thus, the extent of phosphorylation and phospho-ethanolaminylation of the *C. concisus* lipid A was less than that of the *C. jejuni* lipid A, raising the hypothesis that the reduced cytokine and *G. mellonella* response may at least be partly due to the observed differences in lipid A phosphorylation across this genus.

LOS sialylation is another important virulence factor in *C. jejuni* that is associated with enhanced inflammation, increased colonization, and increased risk of developing Guillain-Barré syndrome, the last of which arises due to molecular mimicry between the *C. jejuni* LOS and gangliosides found in peripheral nerves (22, 25, 33, 74). In a previous study we reported the presence of up to two sialic acid residues on the OS of *C. jejuni* isolates and, importantly, increased sialylation was correlated with enhanced TLR4-mediated TNF-α secretion compared with strains without sialic acid (22). Our MS/MS data indicate the absence of sialic acid in the LOS from the four *C. concisus* strains analyzed while confirming NeuAc as part of the reference *C. jejuni* LOS. Furthermore, genomic analyses revealed the lack of sialic acid synthesis capability in all 89 published *C. concisus* genomes. We previously reported nonsialylated LOS produced by some environmental *C. jejuni* isolates (nonlivestock-associated), whereas all human isolates tested were sialic acid-positive (22). Given the significance of sialic acid in the virulence of *C. jejuni*, the absence of sialylation of *C. concisus* LOS is intriguing because it indicates the lack of an important virulence factor that also contributes to inflammatory signaling. An in-depth analysis of the existence of specific LOS biosynthesis gene loci in *C. concisus* as well as the presence of inflammation-associated genes involved in sialic acid and PEA biosynthesis and transfer is warranted to further investigate these important structural differences within the *Campylobacter* genus.

Taken together, our findings show that *C. concisus* isolates exhibit lipid A moieties and heterogeneous OS with overlapping as well as unique features compared with the well-studied *C. jejuni* LOS. Despite many similarities in the LOS structures of these two organisms, differences in the lipid A amidation, fatty acid substituents, and phosphorylation as well as the lack of sialic acid substituents in the *C. concisus* LOS are of significance. The potential association of LOS variations with clinical outcome awaits examination of a larger sample of strains from diverse backgrounds and may give further insight into the remaining question of *C. concisus*' pathogenic potential. Furthermore, it is interesting to speculate that these *Campylobacter* organisms occupy the same ecological niche in the human host as *C. jejuni*, which may result in interspecies cross-talk and a potential indirect effect on *Campylobacter*-related pathogenicity. Our findings on LOS composition, proinflammatory potential, and bacterial virulence provide structural and functional insights into the *C. concisus* LOS that increase our understanding of this underexplored *Campylobacter* species and its role in human disease.

REFERENCES

1. Tanner, A. C. R., J. L. Dzink, J. L. Ebersole, and S. S. Socransky. 1987. *Wolinella recta, Campylobacter concisus, Bacteroides gracilis*, and *Eikeneila corrodens* from periodontal lesions. *J. Periodontal Res.* **22:** 327–330.

2. Deshpande, N. P., N. O. Kaakoush, M. R. Wilkins, and H. M. Mitchell. 2013. Comparative genomics of *Campylobacter concisus* isolates reveals genetic diversity and provides insights into disease association. *BMC Genomics.* **14:** 585.

3. Kaakoush, N. O., and H. M. Mitchell. 2012. *Campylobacter concisus*—a new player in intestinal disease. *Front. Cell. Infect. Microbiol.* **2:** 4.

4. Nielsen, H. L., T. Ejlertsen, J. Engberg, and H. Nielsen. 2013. High incidence of *Campylobacter concisus* in gastroenteritis in North Jutland, Denmark: a population-based study. *Clin. Microbiol. Infect.* **19:** 445–450.

5. Mukhopadhya, I., J. M. Thomson, R. Hansen, S. H. Berry, E. M. El-Omar, and G. L. Hold. 2011. Detection of *Campylobacter concisus* and other *Campylobacter* species in colonic biopsies from adults with ulcerative colitis. *PLoS One.* **6:** e21490.

6. Van Etterijck, R., J. Breynaert, H. Revets, T. Devreker, Y. Vandenplas, P. Vandamme, and S. Lauwers. 1996. Isolation of *Campylobacter concisus* from feces of children with and without diarrhea. *J. Clin. Microbiol.* **34:** 2304–2306.

7. Kaakoush, N. O., N. Castaño-Rodríguez, H. M. Mitchell, and S. M. Man. 2015. Global epidemiology of *Campylobacter* infection. *Clin. Microbiol. Rev.* **28:** 687–720.

8. Zhang, L., M. M. Si, A. S. Day, S. T. Leach, D. A. Lemberg, S. Dutt, M. Stormon, A. Otley, E. V. O'Loughlin, A. Magoffin, et al. 2009. Detection and isolation of *Campylobacter* species other than *C. jejuni* from children with Crohn's disease. *J. Clin. Microbiol.* **47:** 453–455.

9. Man, S. M., N. O. Kaakoush, S. T. Leach, L. Nahidi, H. K. Lu, J. Norman, A. S. Day, L. Zhang, and H. M. Mitchell. 2010. Host attachment, invasion, and stimulation of proinflammatory cytokines by *Campylobacter concisus* and other non-*Campylobacter jejuni Campylobacter* species. *J. Infect. Dis.* **202:** 1855–1865.

10. Nielsen, H. L., J. Engberg, T. Ejlertsen, R. Bücker, and H. Nielsen. 2012. Short-term and medium-term clinical outcomes of *Campylobacter concisus* infection. *Clin. Microbiol. Infect.* **18:** E459–E465.

11. Nielsen, H. L., J. Engberg, T. Ejlertsen, and H. Nielsen. 2013. Clinical manifestations of *Campylobacter concisus* infection in children. *Pediatr. Infect. Dis. J.* **32:** 1194–1198.

12. Akutko, K., and K. Matusiewicz. 2017. *Campylobacter concisus* as the etiologic agent of gastrointestinal diseases. *Adv. Clin. Exp. Med.* **26:** 149–154.

13. Serichantalergs, O., S. Ruekit, P. Pandey, S. Anuras, C. Mason, L. Bodhidatta, and B. Swierczewski. 2017. Incidence of *Campylobacter concisus* and *C. ureolyticus* in traveler's diarrhea cases and asymptomatic controls in Nepal and Thailand. *Gut Pathog.* **9:** 47.

14. François, R., P. P. Yori, S. Rouhani, M. Siguas Salas, M. Paredes Olortegui, D. Rengifo Trigoso, N. Pisanic, R. Burga, R. Meza, G. Meza Sanchez, et al. 2018. The other *Campylobacters*: not innocent bystanders in endemic diarrhea and dysentery in children in low-income settings. *PLoS Negl. Trop. Dis.* **12:** e0006200.

15. Castaño-Rodríguez, N., N. O. Kaakoush, W. S. Lee, and H. M. Mitchell. 2017. Dual role of *Helicobacter* and *Campylobacter* species in IBD: a systematic review and meta-analysis. *Gut.* **66:** 235–249.

16. Ismail, Y., H. Lee, S. M. Riordan, M. C. Grimm, and L. Zhang. 2013. The effects of oral and enteric *Campylobacter concisus* strains on expression of TLR4, MD-2, TLR2, TLR5 and COX-2 in HT-29 cells. *PLoS One.* **8:** e56888.

17. Mukhopadhya, I., R. Hansen, E. M. El-Omar, and G. L. Hold. 2012. IBD—what role do Proteobacteria play? *Nat. Rev. Gastroenterol. Hepatol.* **9:** 219–230.

18. Liu, M., C. M. John, and G. A. Jarvis. 2010. Phosphoryl moieties of lipid A from *Neisseria meningitidis* and *N. gonorrhoeae* lipooligosaccharides play an important role in activation of both MyD88- and TRIF-dependent TLR4-MD-2 signaling pathways. *J. Immunol.* **185:** 6974–6984.

19. Park, B. S., D. H. Song, H. M. Kim, B-S. Choi, H. Lee, and J-O. Lee. 2009. The structural basis of lipopolysaccharide recognition by the TLR4-MD-2 complex. *Nature.* **458:** 1191–1195.

20. Maeshima, N., and R. C. Fernandez. 2013. Recognition of lipid A variants by the TLR4-MD-2 receptor complex. *Front. Cell. Infect. Microbiol.* **3:** 3.

21. Rathinam, V. A. K., D. M. Appledorn, K. A. Hoag, A. Amalfitano, and L. S. Mansfield. 2009. *Campylobacter jejuni*-induced activation of dendritic cells involves cooperative signaling through toll-like receptor 4 (TLR4)-MyD88 and TLR4-TRIF axes. *Infect. Immun.* **77:** 2499–2507.

22. Stephenson, H. N., C. M. John, N. Naz, O. Gundogdu, N. Dorrell, B. W. Wren, G. A. Jarvis, and M. Bajaj-Elliott. 2013. *Campylobacter jejuni* lipooligosaccharide sialylation, phosphorylation, and amide/ester linkage modifications fine-tune human toll-like receptor 4 activation. *J. Biol. Chem.* **288:** 19661–19672.

23. Müller, J., B. Meyer, I. Hänel, and H. Hotzel. 2007. Comparison of lipooligosaccharide biosynthesis genes of *Campylobacter jejuni* strains with varying abilities to colonize the chicken gut and to invade Caco-2 cells. *J. Med. Microbiol.* **56:** 1589–1594.

24. Naito, M., E. Frirdich, J. A. Fields, M. Pryjma, J. Li, A. Cameron, M. Gilbert, S. A. Thompson, and E. C. Gaynor. 2010. Effects of sequential *Campylobacter jejuni* 81–176 lipooligosaccharide core truncations on biofilm formation, stress survival, and pathogenesis. *J. Bacteriol.* **192:** 2182–2192.

25. Louwen, R., A. Heikema, A. Van Belkum, A. Ott, M. Gilbert, W. Ang, H. P. Endtz, M. P. Bergman, and E. E. Nieuwenhuis. 2008. The sialylated lipooligosaccharide outer core in *Campylobacter jejuni* is an important determinant for epithelial cell invasion. *Infect. Immun.* **76:** 4431–4438.

26. Parker, C. T., S. T. Horn, M. Gilbert, W. G. Miller, D. L. Woodward, and R. E. Mandrell. 2005. Comparison of *Campylobacter jejuni* lipooligosaccharide biosynthesis loci from a variety of sources. *J. Clin. Microbiol.* **43:** 2771–2781.

27. Parker, C. T., M. Gilbert, N. Yuki, H. P. Endtz, and R. E. Mandrell. 2008. Characterization of lipooligosaccharide-biosynthetic loci of *Campylobacter jejuni* reveals new lipooligosaccharide classes: Evidence of mosaic organizations. *J. Bacteriol.* **190:** 5681–5689.

28. Moran, A. P., U. Zahringer, U. Seydel, D. Scholz, P. Stutz, and E. T. Rietschel. 1991. Structural analysis of the lipid A component of *Campylobacter jejuni* CCUG 10936 (Serotype O-2) lipopolysaccharide. Description of a lipid A containing a hybrid backbone of 2-amino-2-deoxy-D-glucose and 2,3-diamino-2,3-dideoxy-D-glucose. *Eur. J. Biochem.* **198:** 459–469.

29. Cullen, T. W., J. P. O'Brien, D. R. Hendrixson, D. K. Giles, R. I. Hobb, S. A. Thompson, J. S. Brodbelt, and M. S. Trent. 2013. EptC of *Campylobacter jejuni* mediates phenotypes involved in host interactions and virulence. *Infect. Immun.* **81:** 430–440.

30. van Mourik, A., L. Steeghs, J. Van Laar, H. D. Meiring, H. J. Hamstra, J. P. M. Van Putten, and M. M. S. M. Wösten. 2010. Altered linkage of hydroxyacyl chains in lipid A of *Campylobacter jejuni* reduces TLR4 activation and antimicrobial resistance. *J. Biol. Chem.* **285:** 15828–15836.

31. Dorrell, N., J. A. Mangan, K. G. Laing, J. Hinds, D. Linton, H. Al-Ghusein, B. G. Barrell, J. Parkhill, N. G. Stoker, A. V. Karlyshev, et al. 2001. Whole genome comparison of *Campylobacter jejuni* human isolates using a low-cost microarray reveals extensive genetic diversity. *Genome Res.* **11:** 1706–1715.

32. Kuijf, M. L., J. N. Samsom, W. van Rijs, M. Bax, R. Huizinga, A. P. Heikema, P. A. van Doorn, A. van Belkum, Y. van Kooyk, P. C. Burgers, et al. 2010. TLR4-mediated sensing of *Campylobacter jejuni* by dendritic cells is determined by sialylation. *J. Immunol.* **185:** 748–755.

33. Heikema, A. P., R. I. Koning, S. Duarte dos Santos Rico, H. Rempel, B. C. Jacobs, H. P. Endtz, W. J. B. van Wamel, and J. N. Samsom. 2013. Enhanced, sialoadhesin-dependent uptake of Guillain-Barré syndrome-associated *Campylobacter jejuni* strains by human macrophages. *Infect. Immun.* **81:** 2095–2103.

34. Heikema, A. P., M. P. Bergman, H. Richards, P. R. Crocker, M. Gilbert, J. N. Samsom, W. J. B. Van Wamel, H. P. Endtz, and A. Van Belkum. 2010. Characterization of the specific interaction between sialoadhesin and sialylated *Campylobacter jejuni* lipooligosaccharides. *Infect. Immun.* **78:** 3237–3246.

35. Hansen, R., S. H. Berry, I. Mukhopadhya, J. M. Thomson, K. A. Saunders, C. E. Nicholl, W. M. Bisset, S. Loganathan, G. Mahdi, D. Kastner-Cole, et al. 2013. The microaerophilic microbiota of de-novo paediatric inflammatory bowel disease: the BISCUIT study. *PLoS One.* **8:** e58825.

36. Karlyshev, A. V., D. Linton, N. A. Gregson, and B. W. Wren. 2002. A novel paralogous gene family involved in phase-variable flagella-mediated motility in *Campylobacter jejuni. Microbiology.* **148:** 473–480.

37. Duffy, G., O. A. Lynch, and C. Cagney. 2008. Tracking emerging zoonotic pathogens from farm to fork. *Meat Sci.* **78:** 34–42.

38. Apicella, M. A. 2008. Isolation and characterization of lipopolysaccharides. *Methods Mol. Biol.* **431:** 3–13.

39. Pringle, S. D., K. Giles, J. L. Wildgoose, J. P. Williams, S. E. Slade, K. Thalassinos, R. H. Bateman, M. T. Bowers, and J. H. Scrivens. 2007. An investigation of the mobility separation of some peptide and protein ions using a new hybrid quadrupole / travelling wave IMS / oa-ToF instrument. *Int. J. Mass Spectrom.* **261:** 1–12.

40. Giles, K., S. D. Pringle, K. R. Worthington, D. Little, J. L. Wildgoose, and R. H. Bateman. 2004. Applications of a travelling wave-based radio-frequency-only stacked ring ion guide. *Rapid Commun. Mass Spectrom.* **18:** 2401–2414.

41. Phillips, N. J., C. M. John, and G. A. Jarvis. 2016. Analysis of bacterial lipooligosaccharides by MALDI-TOF MS with traveling wave ion mobility. *J. Am. Soc. Mass Spectrom.* **27:** 1263–1276.

42. Gemmell, M. R., S. Berry, I. Mukhopadhya, R. Hansen, H. L. Nielsen, M. Bajaj-Elliott, H. Nielsen, and G. L. Hold. 2018. Comparative genomics of *Campylobacter concisus*: analysis of clinical strains reveals genome diversity and pathogenic potential. *Emerg. Microbes Infect.* **7:** 116.

43. Chung, H. K. L., A. Tay, S. Octavia, J. Chen, F. Liu, R. Ma, R. Lan, S. M. Riordan, M. C. Grimm, and L. Zhang. 2016. Genome analysis of *Campylobacter concisus* strains from patients with inflammatory bowel disease and gastroenteritis provides new insights into pathogenicity. *Sci. Rep.* **6:** 38442.

44. Zhang, L., V. Budiman, A. S. Day, H. Mitchell, D. A. Lemberg, S. M. Riordan, M. Grimm, S. T. Leach, Y. Ismail. 2010. Isolation and detection of *Campylobacter concisus* from saliva of healthy individuals and patients with inflammatory bowel disease. *J. Clin. Microbiol.* **48:** 2965–2967.

45. Mahendran, V., S. M. Riordan, M. C. Grimm, T. A. T. Tran, J. Major, N. O. Kaakoush, H. Mitchell, and L. Zhang. 2011. Prevalence of *Campylobacter* species in adult Crohn's disease and the preferential colonization sites of *Campylobacter* species in the human intestine. *PLoS One.* **6:** e25417.

46. Ismail, Y., V. Mahendran, S. Octavia, A. S. Day, S. M. Riordan, M. C. Grimm, R. Lan, D. Lemberg, T. A. T. Tran, and L. Zhang. 2012. Investigation of the enteric pathogenic potential of oral *Campylobacter concisus* strains isolated from patients with inflammatory bowel disease. *PLoS One.* **7:** e38217.

47. Mahendran, V., Y. S. Tan, S. M. Riordan, M. C. Grimm, A. S. Day, D. A. Lemberg, S. Octavia, R. Lan, and L. Zhang. 2013. The prevalence and polymorphisms of zonula occluden toxin gene in multiple *Campylobacter concisus* strains isolated from saliva of patients with inflammatory bowel disease and controls. *PLoS One.* **8:** 375525.

48. Seemann, T. 2014. Prokka: rapid prokaryotic genome annotation. *Bioinformatics.* **30:** 2068–2069.

49. Stajich, J. E., D. Block, K. Boulez, S. E. Brenner, S. A. Chervitz, C. Dagdigian, G. Fuellen, J. G. R. Gilbert, I. Korf, H. Lapp, et al. 2002. The Bioperl toolkit: Perl modules for the life sciences. *Genome Res.* **12:** 1611–1618.

50. Tange, O. 2011. GNU parallel: the command-line power tool. ;login. **36:** 42–47.

51. Camacho, C., G. Coulouris, V. Avagyan, N. Ma, J. Papadopoulos, K. Bealer, and T. L. Madden. 2009. BLAST+: architecture and applications. *BMC Bioinformatics.* **10:** 421.

52. Hyatt, D., G. L. Chen, P. F. LoCascio, M. L. Land, F. W. Larimer, and L. J. Hauser. 2010. Prodigal: prokaryotic gene recognition and translation initiation site identification. *BMC Bioinformatics.* **11:** 119.

53. Laslett, D., and B. Canback. 2004. ARAGORN, a program to detect tRNA genes and tmRNA genes in nucleotide sequences. *Nucleic Acids Res.* **32:** 11–16.

54. Finn, R. D., J. Clements, and S. R. Eddy. 2011. HMMER web server: interactive sequence similarity searching. *Nucleic Acids Res.* **39:** W29–W37.

55. Kolbe, D. L., and S. R. Eddy. 2011. Fast filtering for RNA homology search. *Bioinformatics.* **27:** 3102–3109.

56. Lagesen, K., P. Hallin, E. A. Rødland, H. H. Stærfeldt, T. Rognes, and D. W. Ussery. 2007. RNAmmer: consistent and rapid annotation of ribosomal RNA genes. *Nucleic Acids Res.* **35:** 3100–3108.

57. Petersen, T. N., S. Brunak, G. Von Heijne, and H. Nielsen. 2011. SignalP 4.0: discriminating signal peptides from transmembrane regions. *Nat. Methods.* **8:** 785–786.

58. Kanehisa, M., Y. Sato, and K. Morishima. 2016. BlastKOALA and GhostKOALA: KEGG tools for functional characterization of genome and metagenome sequences. *J. Mol. Biol.* **428:** 726–731.

59. John, C. M., M. Liu, and G. A. Jarvis. 2009. Natural phosphoryl and acyl variants of lipid A from *Neisseria meningitidis* strain 89I differentially induce tumor necrosis factor-α in human monocytes. *J. Biol. Chem.* **284:** 21515–21525.

60. Harding, C. R., G. N. Schroeder, J. W. Collins, and G. Frankel. 2013. Use of *Galleria mellonella* as a model organism to study *Legionella pneumophila* infection. *J. Vis. Exp.* e50964.

61. Champion, O. L., A. V. Karlyshev, N. J. Senior, M. Woodward, R. La Ragione, S. L. Howard, B. W. Wren, and R. W. Titball. 2010. Insect infection model for *Campylobacter jejuni* reveals that *O*-methyl phosphoramidate has insecticidal activity. *J. Infect. Dis.* **201:** 776–782.

62. Dzieciatkowska, M., D. Brochu, A. Van Belkum, A. P. Heikema, N. Yuki, R. S. Houliston, J. C. Richards, M. Gilbert, and J. Li. 2007. Mass spectrometric analysis of intact lipooligosaccharide: direct evidence for *O*-acetylated sialic acids and discovery of *O*-linked glycine expressed by *Campylobacter jejuni*. *Biochemistry.* **46:** 14704–14714.

63. Dzieciatkowska, M., X. Liu, A. P. Heikema, R. S. Houliston, A. Van Belkum, E. K. H. Schweda, M. Gilbert, J. C. Richards, and J. Li. 2008. Rapid method for sensitive screening of oligosaccharide epitopes in the lipooligosaccharide from *Campylobacter jejuni* strains isolated from Guillain-Barré syndrome and Miller Fisher syndrome patients. *J. Clin. Microbiol.* **46:** 3429–3436.

64. Szymanski, C. M., F. St. Michael, H. C. Jarrell, J. Li, M. Gilbert, S. Larocque, E. Vinogradov, and J. R. Brisson. 2003. Detection of conserved N-linked glycans and phase-variable lipooligosaccharides and capsules from *Campylobacter* cells by mass spectrometry and high resolution magic angle spinning NMR spectroscopy. *J. Biol. Chem.* **278:** 24509–24520.

65. Caroff, M., and D. Karibian. 2003. Structure of bacterial lipopolysaccharides. *Carbohydr. Res.* **338:** 2431–2447.

66. Richards, V. P., T. Lefébure, P. D. Pavinski Bitar, and M. J. Stanhope. 2013. Comparative characterization of the virulence gene clusters (lipooligosaccharide [LOS] and capsular polysaccharide [CPS]) for *Campylobacter coli*, *Campylobacter jejuni* subsp. *jejuni* and related *Campylobacter* species. *Infect. Genet. Evol.* **14:** 200–213.

67. Brandenburg, K., and U. Seydel. 2010. Conformation and supramolecular structure of lipid A. *Adv. Exp. Med. Biol.* **667:** 25–38.

68. Aspinall, G. O., A. G. McDonald, and H. Pang. 1992. Structures of the O chains from lipopolysaccharides of *Campylobacter jejuni* serotypes O:23 and O:36. *Carbohydr. Res.* **231:** 13–30.

69. Penner, J. L., and G. O. Aspinall. 1997. Diversity of lipopolysaccharide structures in *Campylobacter jejuni*. *J. Infect. Dis.* **176(Suppl 2):** S135–S138.

70. Karlyshev, A. V., D. Linton, N. A. Gregson, A. J. Lastovica, and B. W. Wren. 2000. Genetic and biochemical evidence of a *Campylobacter jejuni* capsular polysaccharide that accounts for Penner serotype specificity. *Mol. Microbiol.* **35:** 529–541.

71. Scott, N. E., H. Nothaft, A. V. G. Edwards, M. Labbate, S. P. Djordjevic, M. R. Larsen, C. M. Szymanski, and S. J. Cordwell. 2012. Modification of the *Campylobacter jejuni* N-linked glycan by EptC protein-mediated addition of phosphoethanolamine. *J. Biol. Chem.* **287:** 29384–29396.

72. Cullen, T. W., and M. S. Trent. 2010. A link between the assembly of flagella and lipooligosaccharide of the Gram-negative bacterium *Campylobacter jejuni*. *Proc. Natl. Acad. Sci. USA.* **107:** 5160–5165.

73. John, C. M., M. Liu, N. J. Phillips, Z. Yang, C. R. Funk, L. I. Zimmerman, M. Griffiss, D. C. Stein, and G. A. Jarvis. 2012. Lack of lipid A pyrophosphorylation and functional *lptA* reduces inflammation by *Neisseria* commensals. *Infect. Immun.* **80:** 4014–4026.

74. Mortensen, N. P., M. L. Kuijf, C. W. Ang, P. Schiellerup, K. A. Krogfelt, B. C. Jacobs, A. van Belkum, H. P. Endtz, and M. P. Bergman. 2009. Sialylation of *Campylobacter jejuni* lipo-oligosaccharides is associated with severe gastro-enteritis and reactive arthritis. *Microbes Infect.* **11:** 988–994.